

Allylphenoxy piperidinium halides as corrosion inhibitors of carbon steel and biocides

Gunay MEHDIYEVA MUZAKIR*^{ORCID}, Musa BAIRAMOV RZA^{ORCID},
Shahnaz HOSSEINZADEH BAHADOR^{ORCID}, Gulnara HASANOVA MUSA^{ORCID}
Department of Chemistry, Faculty of Chemistry, Baku State University, Baku, Azerbaijan

Received: 09.01.2020

Accepted/Published Online: 27.03.2020

Final Version: 01.06.2020

Abstract: A series of 1-(4-(2-allylphenoxy)butyl)piperidin-1-ium halides (**4a-d**) was synthesized and characterized via spectroscopic methods (FTIR, ¹H NMR). The corrosion inhibition of the synthesized halides on carbon steel in water-salt-hydrocarbon environment, saturated with H₂S, was investigated. For this purpose, a series of techniques such as gravimetric measurement, potentiodynamic polarisation, and scanning electron microscope (SEM) were used and some thermodynamic parameters of corrosion process ($\Delta G_{ads.}$, $\Delta H_{ads.}^0$, $\Delta S_{ads.}^0$) were evaluated. The steel surface was checked by SEM, and the steel surface showed good surface coverage. The results showed that the synthesized compounds at the concentrations 125, 150 mg × L⁻¹ have corrosion inhibition activity of 78%–95% by gravimetric measurements and 81%–92% by potentiodynamic measurements at 100, 150 mg × L⁻¹. The biological activity was examined against sulphate-reducing bacteria (SRB). It was revealed that at the concentration of compounds **4c** and **4d**, 100 mg × L⁻¹, the antibacterial activity was 100%.

Key words: Piperidinium halides, phenolic compounds, corrosion inhibitors, adsorption, biocides

1. Introduction

The protection of different equipment from corrosion is one of the most important ecological and economic problems of petrochemistry, especially in environments containing hydrogen sulphide, CO₂, salt, and other substances [1–5]. Moreover, the corrosion of metal constructions in oil, gas and gas condensate fields due to sulphate-reducing bacteria (SRB), which is mainly carried out with the formation of hydrogen sulphide and other sulphides [6–10], is a serious problem.

It is worth noting that a large number of organic compounds with anticorrosive, bactericidal, and other properties have been discovered [11–26]. While using such compounds as corrosion inhibitors, the following can be observed: the formation of chemisorbed layers on the metal surface and a sharp decrease in the rate of corrosion. Although the various corrosion inhibitors comprising structure functional fragments and heteroatoms (O, N, S, P) are known [27], organic compounds with anticorrosive and bactericidal (SRB) properties are very limited [8,28]. Therefore, it is crucial to work towards discovering new corrosion inhibitors with these characteristics.

It is worth noting that alkenylphenol and their derivatives are functionally substituted organic compounds [29–42] that can be applied as effective corrosion inhibitors and biocides [28, 43–45]. Furthermore, such compounds can be used as light stabilisers for polymers [46], additives in mineral oils and fuels [47–49], to

*Correspondence: mehdiyeva_gm@mail.ru

obtain photo-resisting materials [50,51]. Cationic forms of alkenylphenol derivatives are especially important as corrosion inhibitors and biocides, as they are highly soluble in water [28,44].

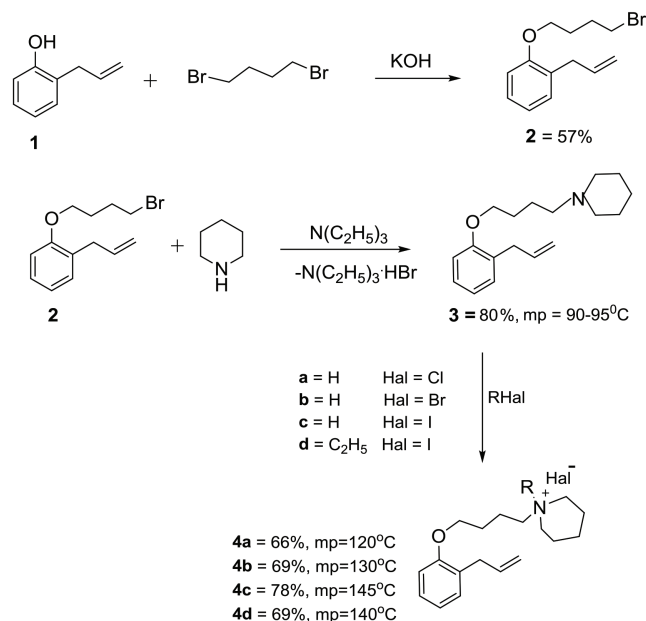
This paper aims to discover new corrosion inhibitors through the synthesis of new allylphenol derivatives containing nitrogen, halides, and unsaturated fragments in their structures. This will be accomplished by studying these new allylphenol derivatives as biocides and inhibitors of the hydrogen-sulphide corrosion of St.3 steel, employing gravimetric (25 °C, 35 °C, and 45 °C) and electrochemical (25 °C) methods in systems comprising a 3% aqueous solution of NaCl and hydrocarbons (kerosene) (water: kerosene = 9:1 vol.) saturated with hydrogen sulphide. The thermodynamic parameters (ΔG , ΔH , and ΔS) of corrosion in identical conditions in the presence of synthesized inhibitors were determined.

2. Materials and methods

2.1. Synthesis

2.1.1. Synthesis of 1-allyl-2-(4-bromobutoxy)benzene (2)

1-allyl-2-(4-bromobutoxy)benzene (**2**) was obtained [52] by interaction of 13.4 g (0.1 mol) 2-allylphenol (Aldrich) (**1**) with 43.2 g (0.2 mol) 1,4-dibromobutane (Aldrich) in 2-propanol (as a solvent) (Karmalab) in the presence of 5.6 g (0.1 mol) KOH (Karmalab). The reaction carried out at 80 °C for 1.5 h (Scheme). bp = 130 °C /5 mm, $n_D^{20} = 1.530$, $d_4^{20} = 1.242 \text{ g} \times \text{cm}^{-3}$.



Scheme The structures of the synthesized compounds **4a-d**.

2.1.2. Synthesis of 1-(4-(2-allylphenoxy)butyl) piperidine (3)

1-(4-(2-Allylphenoxy)butyl) piperidine (**3**) was obtained by a reaction of equimolar of 1-allyl-2-(4-bromobutoxy)benzene (**2**) amounts and piperidine (Karmalab) in the presence of triethylamine (Karmalab) (Scheme). The reaction was carried out at 25 °C for 24 h. The obtained mixture was filtered and dried with Na_2SO_4 (ECOS). It was then distilled under high vacuum due to separate unreacted starting reagents.

2.1.3. Synthesis of ammonium salts 4a-d

Piperidinium halides (**4a-d**) were prepared with a reaction of equimolar amounts 1-(4-(2-allylphenoxy)butyl) piperidine (**3**) with hydrogen halides (HCl, HBr, and HI) and ethyl iodide at 30 °C–40 °C for a reaction period 0.5 h. Hydrogen halides were obtained by the reaction of NaCl, KBr, KI (Karmalab) with sulfuric acid (Karmalab). The obtained 1-(4-(2-allylphenoxy)butyl)-piperidin-1-ium chloride (**4a**), 1-(4-(2-allylphenoxy)butyl)-piperidin-1-ium bromide (**4b**), 1-(4-(2-allylphenoxy)butyl)-piperidin-1-ium iodide (**4c**) and 1-(4-(2-allylphenoxy)butyl)-1-ethylpiperidin-1-ium iodide (**4d**) (Scheme) were recrystallised several times from water and then dried under vacuum.

The structure of the prepared compounds **4a**, **b**, **d** and compound **2,3** were confirmed by the FTIR and ¹H NMR spectroscopy method. For the FTIR analysis, “Varian 3600 FTIR” were used for NMR-spectroscopy–BRUKER FT NMR spectrometer AVANCE 300 (300 MHz) with a BVT 3200 variable temperature unit in 5-mm sample tubes, using Bruker Standard software (solvent–D₂O, CDCl₃).

2.2. Gravimetric corrosion tests

The gravimetric measurements were carried out at 25 °C, 35 °C, and 45 °C for 5 h in a mixture of 3% NaCl water solution and kerosene (9:1 v/v), saturated with hydrogen sulphide; the volume of the mixture was 1 L and concentrations of the inhibitors used were in the range of 50–150 mg × L⁻¹. Further, the rectangular (3.5 cm × 2 cm × 0.2 cm) steel samples were grazed with emery paper, washed with bidistilled water, degreased with acetone and ethanol, and dried at room temperature. After tests, the steel samples were washed again with bidistilled water, degreased with acetone and ethanol, dried and then weighed.

The corrosion rate (K_w (g × m⁻² × h⁻¹)), inhibition effectiveness (η_w , %), and surface coverage (θ) of the steel were determined both in the absence and presence of inhibitors **4a-d** at various concentrations, using Equations (1), (2), and (3) [19,28]:

$$K_W = \frac{W_1 - W_2}{S \times t} \quad (1)$$

$$\eta_W = \left[\frac{K_{Wcorr.} - K_{Wcorr.(inh.)}}{K_{Wcorr.}} \right] \times 100\% \quad (2)$$

$$\theta = \frac{K_{Wcorr.} - K_{Wcorr.(inh.)}}{K_{Wcorr.}} \quad (3)$$

where K_{Wcorr} and $K_{Wcorr(inh.)}$ are the corrosion rates in the absence and presence of inhibitor respectively, and W_1 and W_2 are weight losses of carbon steel in the absence and presence of the inhibitors, respectively.

2.3. Electrochemical measurements

Electrochemical corrosion studies were carried out on the Autolab PGSTAT 30 (Eco-Chemie, Netherlands) potentiostat, with 0.7 cm² silver chloride electrode and platinum electrodes. The data obtained was processed using the GPES software. The above-described NaCl-water/kerosene-hydrogen sulphide mixture was used as a model solution at 25 °C, without stirring [11], while the concentration of the tested compounds varied from 50 to 150 mg × L⁻¹. The inhibition effectiveness (η_p , %) and surface coverage (θ) of steel corrosion were calculated by Equations (4) and (5):

$$\eta_p = \left[\frac{i_{corr.} - i_{corr.(inh.)}}{i_{corr.}} \right] \times 100\% \quad (4)$$

$$\theta = \frac{i_{corr.} - i_{corr.(inh.)}}{i_{corr.}} \quad (5)$$

where $i_{corr.(inh.)}$ and $i_{corr.}$ are the corrosion current density values in the presence and absence of inhibitor, respectively.

2.4. Scanning electron microscopy (SEM)

The surface morphology of the steel samples before and after the immersion was studied using the SEM-XL-30 microscope at the concentration of the inhibitors **4a-d** 100 mg \times L⁻¹ for 5 h in a mixture of 3% NaCl water solution and kerosene (9:1 v/v) saturated with hydrogen sulphide.

2.5. Biological activity tests

Antimicrobial activity of the synthesized compounds against SRB was studied at various concentrations (50, 75, 100, 150 and 200 mg \times L⁻¹) of **4a-d** using the method described in the literature [53]. Accordingly, compounds **4a-d** were examined in water media containing SRB microorganisms (10⁴–10⁶ cells in 1 mL), which were taken from the oilfield “Chirag” (Baku, Azerbaijan). 3 mL from the prepared samples of SRB water solutions and studied compounds **4a-d** were added to Postgate medium and were incubated for 15 days at 32 °C. After the incubation period, the concentration of hydrogen sulphide was determined. The control tests were carried out similarly, but without **4a-d**. The degree of inhibition of SRB growth (S, %) was determined by Equation (6):

$$S, \% = \frac{C_1 - C_2}{C_1} \times 100\% \quad (6)$$

where C_1 and C_2 are concentrations (mg \times L⁻¹) of hydrogen sulphide in control and inspected samples before and after incubation period, respectively.

3. Results and discussion

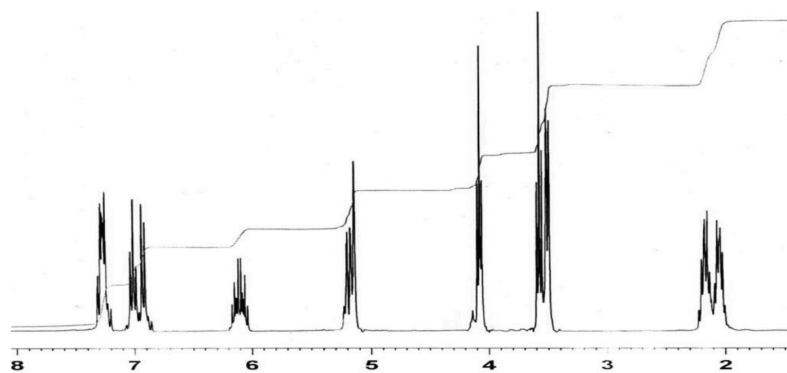
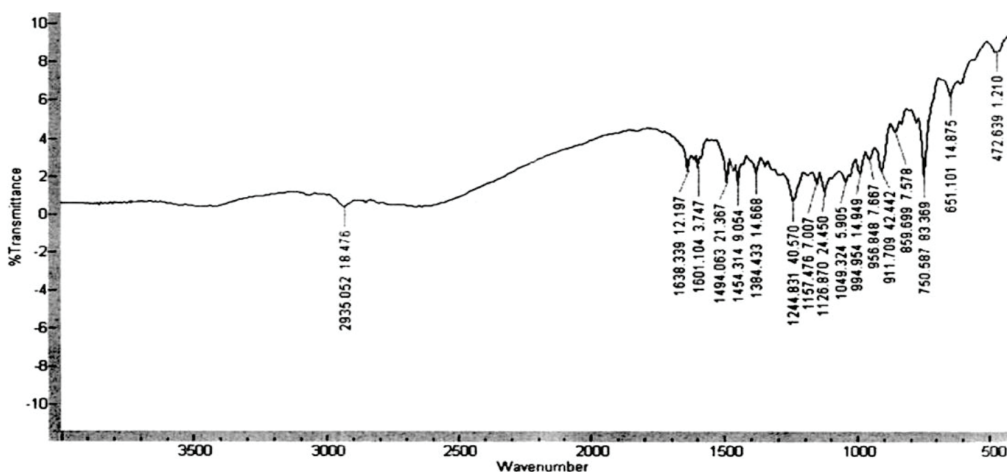
3.1. Characterization of the synthesized compounds

Quaternary piperidinium halides **4a-d** were obtained by the reaction of 1-(4-(2-allylphenoxy) butyl) piperidine (**3**) with halides (HCl, HBr, HI, and ethyl iodide) (Scheme). It was revealed that the yields (66%–78%) and melting points (120 °C–145 °C) of the obtained compounds **4a-d** vary, depending on the nature of the halide taken.

In our previous studies, it was shown that the length of the spacer (the length of the –CH₂ group in the structure of dibromoalkane) affects the yield of the product [44,52]. Therefore, in our future studies, the syntheses were carried out using 1,4-dibromobutane. The formation of precursor compound **2** – 1-allyl-2-(4-bromobutoxy)benzene and **3** – 1-(4-(2-allylphenoxy) butyl) piperidine, and compounds **4a-d** were confirmed by FTIR and NMR spectroscopy.

¹H NMR-spectra of **2** (CDCl₃; δ , ppm) (Figure 1): 1.95–2.2 m (Br-CH₂-CH₂-CH₂-CH₂-O); 3.5 d (Ar-CH₂-CH=CH₂); 3.57 t (Br-CH₂-); 4.1 t (–CH₂-O-); 5.16 m (CH₂=); 6.1 m (–CH₂-CH=CH₂); 6.95 m (C-H-arom); 7.25 d (C-H-arom).

FTIR of compound **3** (Figure 2) showed the following absorption bands at 750 cm⁻¹ (1,2 – substituted aromatic ring); 1244 cm⁻¹ (C-O-deformation), 1494, 1601 cm⁻¹ (C=C-arom), 3070 cm⁻¹ (C-H-arom.); 1638 cm⁻¹ (CH₂=CH); 2935, 2970 cm⁻¹ (CH₂), and 1126 (C-N-stretching), as expected.

Figure 1. ^1H NMR spectra of **2**.Figure 2. FTIR spectra of **3**.

FTIR of **4a** (Figure 3) showed the different absorption bands at 766 cm^{-1} (1,2-substituted aromatic ring); $1257, 1026\text{ cm}^{-1}$ (Ar-O-C); $1498, 1473, 1451, 2935\text{ cm}^{-1}$ (CH_2); 3071 cm^{-1} (C-H-arom); 1599 cm^{-1} (C=C-arom); 1636 cm^{-1} ($\text{CH}_2 = \text{CH}-$); 1130 cm^{-1} (C-N stretching); 2485 cm^{-1} (N^+H).

FTIR of **4b** (Figure 3) showed the following absorption bands at 766 cm^{-1} (1,2-substituted aromatic ring); $1253, 1026\text{ cm}^{-1}$ (Ar-O-C); $2929, 1497, 1452\text{ cm}^{-1}$ (CH_2); 3071 cm^{-1} (C-H-arom); 1599 cm^{-1} (C=C-arom); 1635 cm^{-1} ($\text{CH}_2 = \text{CH}-$); 1131 cm^{-1} (C-N- stretching), $2500, 2610\text{ cm}^{-1}$ (N^+H).

FTIR of **4d** (Figure 3) showed that at 759 cm^{-1} (1,2-substituted aromatic ring); $1238, 1022$ (Ar-O-C); $2941, 1493, 1451$ (CH_2, CH_3); 3055 cm^{-1} (C-H-arom); 1597 cm^{-1} (C=C-arom); 3478 cm^{-1} (C-H-stretching); 1238 (C-N- stretching).

^1H NMR of **4b** (D_2O ; δ , ppm) (Figure 4): 1.5 m (2H, CH_2); 2.85 d (2H, CH_2Ar); 3.05 t (2H, CH_2N); 3.75 t (2H, CH_2O); 5.1 m (2H, $=\text{CH}_2$); 5.7 m (1H, $=\text{CH}$); 6.4–6.9 m (4H, C_6H_4), 8.7 s (1H, ^+NH).

The results of the spectral characteristics confirmed the structure of the precursor compounds (**2,3**) and the synthesized (**4a,b,d**) compounds. In Figure 3, all the prepared compounds have the same absorption bands. The only difference is in the absorption band of **4d**, owing to the presence of methyl group bands and $^+\text{NR}_4$ in the structure. While comparing the ^1H NMR spectra of compound **2** and **4d** (Figure 1 and 4), it can be

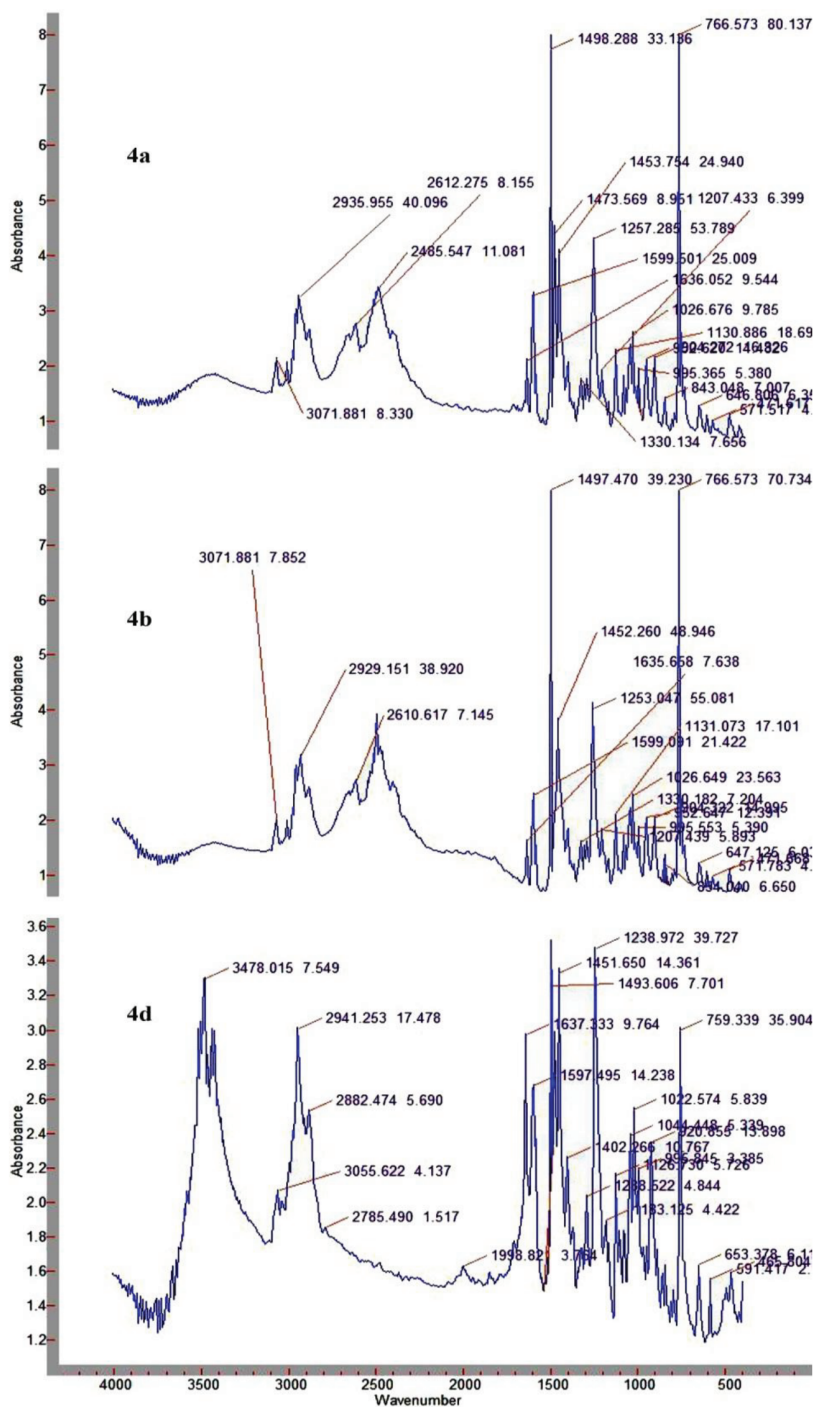


Figure 3. FTIR spectra of 4a, b, d.

seen that the CH₂-Br signals have disappeared and replaced by the signals of the ammonium fragment, and also ⁺N-H in a weak field (8.7) appeared. While comparing the FTIR spectra of compound 3 (Figure 2) with compounds 4a,b (Figure 3), it can be seen that the absorption band of the quaternary ammonium salt appeared in spectra of 4a,b.

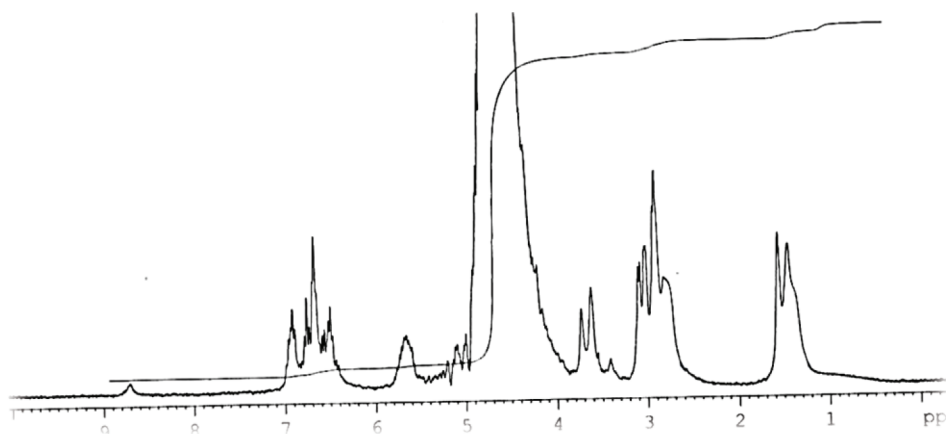


Figure 4. ^1H NMR spectra of **4b**.

3.2. Gravimetric measurements

Organic compounds containing nitrogen, sulphur, oxygen, aromatic rings, as well as various multiple bonds in their structures are effective corrosion inhibitors, especially in acidic environments [54,55]. These compounds, due to the functional groups in the structures, are well adsorbed on the metal surface. Among these compounds are functionally substituted organic compounds based on alkenylphenol, which have higher corrosion inhibition properties in aggressive environments [28,29,44]. Moreover, in the presence of quaternary ammonium fragments in their structures, their inhibitory properties increase due to their good solubility in water [28].

Considering all these points, it was interesting to study of the synthesized **4a-d** as corrosion inhibitors of steel St.3 in a mixture of 3% NaCl water solution and kerosene (9:1 v/v) saturated with hydrogen sulphide.

The obtained results (Table 1) demonstrated that the studied organic compounds **4a-d** have inhibition effectiveness at various temperatures (25 °C, 35 °C, and 45 °C) and concentrations (50, 75, 100, 125, 150 mg $\times\text{L}^{-1}$). Table 1 also shows that among the inhibitors compound, **4a** has a relatively low protection degree. This can be explained based on the structure of the compound containing the chloride anion. Compounds **4b** and **4d** (150 mg $\times\text{L}^{-1}$), containing bromide and iodide ions in the structures, had the best corrosion inhibition effectiveness as expected. Moreover, as it can be seen, the protection of steel was 93%–95% at 25 °C, 70%–72% at 35 °C, and 66%–68% at 45 °C. Compound **4c** had a small difference in corrosion inhibition efficiency degree of protection (92% at the concentration 150 mg $\times\text{L}^{-1}$) compared with **4b** and **4d**.

Furthermore, the results of the studies show that compounds **4b** and **4d** at the concentration 150 mg $\times\text{L}^{-1}$ have high inhibition properties and that the studied inhibitors, due to their properties, are not inferior to corrosion inhibitors, which are known in the literature [8], and in some cases even surpassed them [1].

3.3. Potentiodynamic polarization studies

The potentiodynamic polarization studies (Figure 5) revealed a shift in currents. With an increase in concentration of **4a-d**, the corrosion potential shifts towards positive values. This can be the result of the adsorption of the tested compounds on the surface of the steel electrode. In this case, the rate of redox reactions slows down, and inhibition of corrosion process occurs. Notably, the comparison of the results of electrochemical and gravimetric studies conducted at 25 °C makes it possible to identify the correlation.

Table 1. Corrosion rate (K), surface coverage (θ), and corrosion inhibition effectiveness (η_w , %) determined by gravimetric measurements at various temperatures for carbon steel.

Inhibitor	Conc., mg \times L ⁻¹	$K_T = 25^\circ C$, g(m ² \times h) ⁻¹	$K_T = 35^\circ C$, g(m ² \times h) ⁻¹	$K_T = 45^\circ C$, g(m ² \times h) ⁻¹	$\theta_T = 25^\circ C$	$\theta_T = 35^\circ C$	$\theta_T = 45^\circ C$	$\eta_T = 25^\circ C$, %	$\eta_T = 35^\circ C$, %	$\eta_T = 45^\circ C$, %
4a	50	2.394	4.062	4.357	0.46	0.20	0.18	46	20	18
	75	1.862	-	-	0.58	-	-	58	-	-
	100	1.374	3.148	3.560	0.69	0.38	0.33	69	38	33
	125	0.975	-	-	0.78	-	-	78	-	-
	150	0.709	2.234	2.657	0.84	0.56	0.50	84	56	50
4b	50	1.723	3.402	3.985	0.61	0.33	0.25	61	33	25
	75	1.374	-	-	0.69	-	-	69	-	-
	100	0.842	2.184	2.604	0.81	0.57	0.51	81	57	51
	125	0.532	-	-	0.88	-	-	88	-	-
	150	0.310	1.523	1.807	0.93	0.70	0.66	93	70	66
4c	50	1.596	3.351	3.826	0.64	0.34	0.28	64	34	28
	75	1.197	-	-	0.73	-	-	73	-	-
	100	0.754	2.285	2.657	0.83	0.55	0.50	83	55	50
	125	0.576	-	-	0.87	-	-	87	-	-
	150	0.355	1.625	1.860	0.92	0.68	0.65	92	68	65
4d	50	1.285	3.148	3.879	0.71	0.38	0.27	71	38	27
	75	0.797	-	-	0.82	-	-	82	-	-
	100	0.576	1.930	2.391	0.87	0.62	0.55	87	62	55
	125	0.399	-	-	0.91	-	-	91	-	-
	150	0.222	1.422	1.700	0.95	0.72	0.68	95	72	68
Without inhibitor	-	4.33	5.07	5.314	-	-	-	-	-	-

The obtained values of the corrosion current densities ($i_{corr.}$), Tafel slopes (β_c, β_a), corrosion rate (K), surface coverage (θ), and percentage of inhibition effectiveness ($\eta_p, \%$) of the synthesized compounds are given in Table 2. These data demonstrate that the studied inhibitors shift the corrosion potential ($E_{corr.}$) into the cathodic direction. The cathodic Tafel slopes (β_c) and anodic Tafel slopes (β_a) values depend on the concentration of **4a-d**. Among the investigated substances, high corrosion effectiveness was exhibited by substances **4b**, **4c**, and **4d** at concentrations 100–150 mg \times L⁻¹ with inhibition effectiveness as 68%–92%.

The results of anticorrosion studies showed that the studied inhibitors are not inferior to the inhibitors described in the literature in terms of anticorrosion properties [3–5].

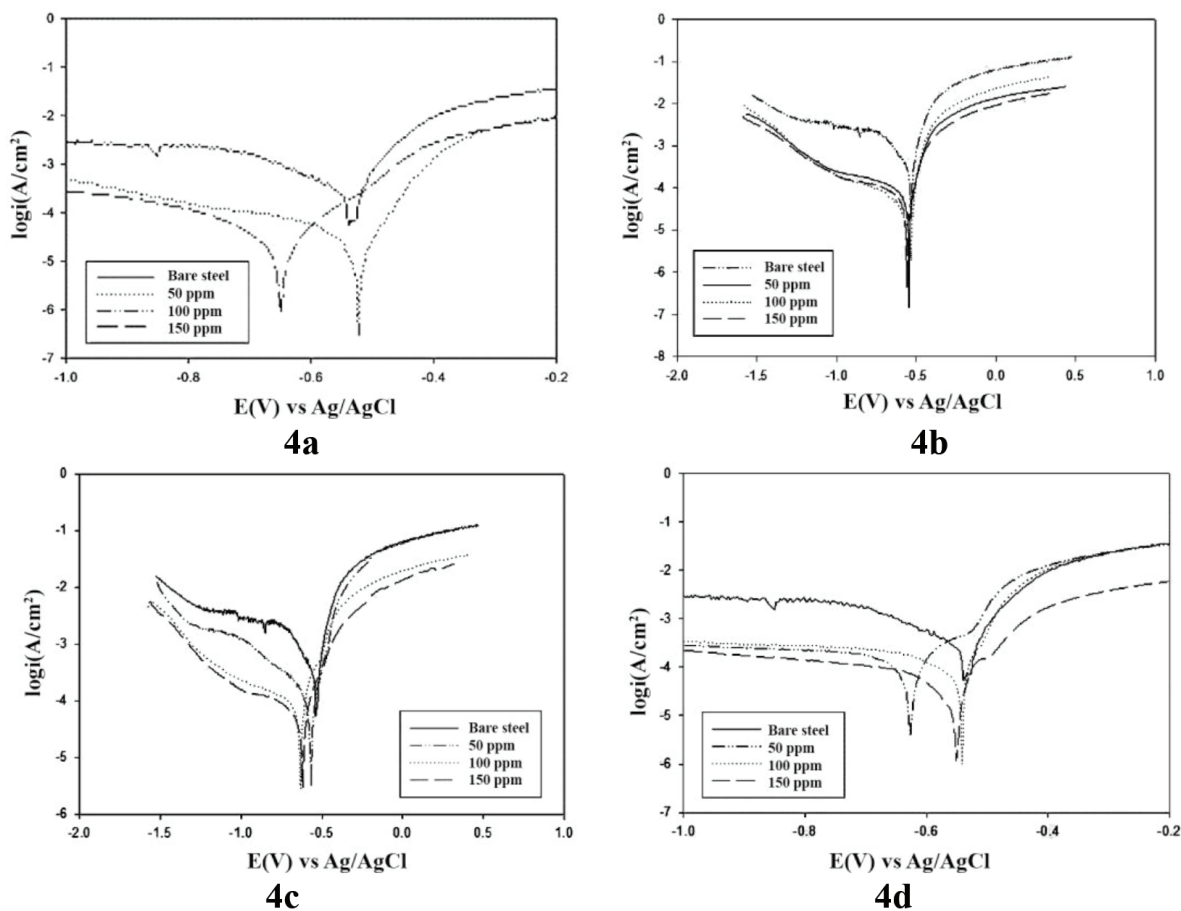


Figure 5. Polarization curves of carbon steel in the model system saturated with H₂S and containing **4a-d** at the different concentrations.

3.4. Adsorption isotherm and thermodynamic data

The analysis of adsorption isotherms can provide basic information on the interaction of an inhibitor with a metal surface [11]. Therefore, the adsorption ability on the metal surface was studied. The surface coverage values (θ) were determined at different concentrations of **4a-d** from gravimetric measurements (Figure 6).

The plots C/θ versus C (Figure 6) are linear with correlation coefficients 0.9972, 0.9919, 0.9983, and 0.9991, respectively. In this case, the adsorption of indicators on the carbon steel surface obeys the Langmuir

adsorption isotherm by Equation (7):

$$\frac{C}{\theta} = C + \frac{1}{K_{ads}} \quad (7)$$

where C is the inhibitor concentration, θ is the degree of coverage on the metal surface and K_{ads} is the equilibrium constant for adsorption desorption process, calculated by the reciprocal of the intercept of isotherm line at various temperatures (Table 3).

Table 2. Results of the potentiodynamic polarization study of carbon steel at 25 °C.

Inhibitor	Conc. of inh., mg $\times L^{-1}$	E, V	I, $\mu A cm^{-2}$	β_c	β_a	R_p, Ω $\times sm^{-2}$	θ	$\eta_p, \%$
4a	50	-0.62	78	0.13	0.06	234	0.40	40
	100	-0.54	71	0.37	0.03	160	0.45	45
	150	-	-	-	-	-	-	-
4b	50	-0.54	42	0.17	0.07	513	0.68	68
	100	-0.55	24	0.17	0.10	611	0.82	82
	150	-0.57	10	0.03	0.04	701	0.92	92
4c	50	-0.57	34	0.04	0.07	357	0.74	74
	100	-0.63	25	0.07	0.04	412	0.81	81
	150	-0.62	20	0.06	0.04	557	0.85	85
4d	50	-0.62	25	0.12	0.09	887	0.81	81
	100	-0.55	16	0.11	0.06	1066	0.88	88
	150	-0.56	11	0.07	0.06	1191	0.92	92
Without inhibitor	-	-0.54	130	0.03	0,05	64	-	-

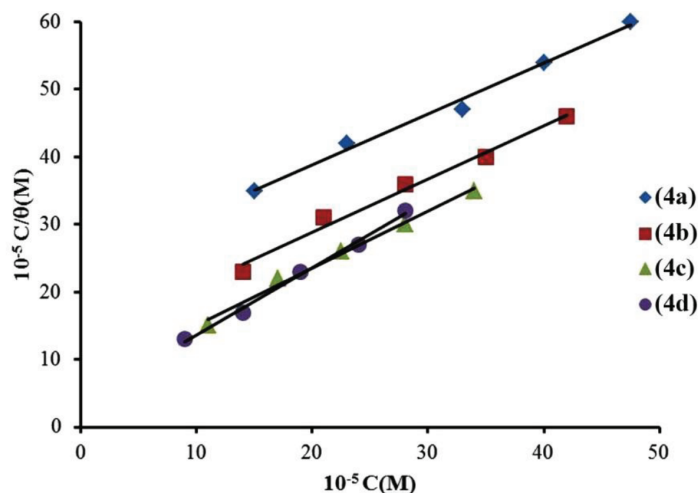


Figure 6. Langmuir adsorption plots for carbon steel at different concentrations of **4a-d** at 25 °C.

It was found that the values of the equilibrium constant decrease with increasing temperature. The high values of K_{ads} ($4.11 \cdot 10^3 M^{-1}$, $7.65 \cdot 10^3 M^{-1}$, $13.40 \cdot 10^3 M^{-1}$, and $21.47 \cdot 10^3 M^{-1}$ for compounds **3a**, **3b**, **3c**, and **3d**, respectively at 25 °C) reflect the high adsorption ability of the inhibitors on the carbon steel surface.

Table 3. Thermodynamic parameters of the inhibitor **4a-d** adsorption on the surface of carbon steel in the presence of hydrogen sulphide, at different temperatures and concentrations.

Inhibitor	Temperature (°C)	K_{ads} ($\times 10^3 M^{-1}$)	ΔG_{ads} , $kJ \times mol^{-1}$	ΔH_{ads} , $kJ \times mol^{-1}$	ΔS_{ads} , $J mol^{-1} \times K^{-1}$
4a	25	4.11	-30.57	-50.53	66.99
	35	1.29	-28.62		71.12
	45	1.15	-29.25		66.90
4b	25	7.65	-32.11	-53.46	71.66
	35	3.03	-30.82		73.52
	45	1.98	-30.68		71.62
4c	25	13.40	-33.49	-55.36	73.37
	35	4.56	-31.86		76.30
	45	3.31	-32.05		73.31
4d	25	21.47	-34.66	-71.87	124.89
	35	6.18	-32.64		127.39
	45	3.48	-32.18		124.83

Table 4. Antimicrobial activity of **4a-d** against SRB.

Inhibitors	The degree (%) of inhibition of growth of SRB at the concentration of inhibitors, $mg \times L^{-1}$				
	50	75	100	150	200
4a	45	62	71	79	89
4b	81	90	96	100	100
4c	88	94	100	100	100
4d	91	95	100	100	100

The free energy (ΔG_{ads}) of adsorption can be calculated by Equation 8:

$$\Delta G_{ads} = -RT \ln(55.5K_{ads}) \quad (8)$$

where ΔG_{ads} is the free energy of adsorption, K_{ads} is the equilibrium constant, T is the absolute temperature, and 55.5 is the molar concentration of water.

The negative values of ΔG_{ads} . (-30.57, -32.11, -33.49, and -34.66 $kJ \times mol^{-1}$ for **3a**, **3b**, **3c**, and **3d**, respectively) indicate spontaneous adsorption of the prepared surfactants on the carbon steel surface.

The ΔH_{ads} values (-50.53, -53.46, -55.36, -71.87 $kJ \times mol^{-1}$ for inhibitors **3a**, **3b**, **3c**, and **3d**, respectively) were calculated using K_{ads} . at respective temperatures. The ΔH_{ads} values indicate that the adsorption in hydrogen sulphide area is an exothermic process. Entropy of the inhibitors' adsorption (ΔS_{ads}) was calculated by Equation (9):

$$\Delta G_{ads} = \Delta H_{ads} - T\Delta S_{ads} \quad (9)$$

The positive values of ΔS_{ads} (66.99, 71.66, 73.37, 124.89 $J \times mol^{-1} \times K^{-1}$ for inhibitors **3a**, **3b**, **3c**, and **3d**, respectively) are possibly related to an increase in disorder due to the adsorption of the studied molecules and desorption of water molecules.

3.5. Scanning electron microscopy (SEM)

To test the inhibitory properties of organic compounds, the morphology of the metal surface is important [8]. For this purpose, the surface morphology of steel in the absence and presence of inhibitors **4a-d** after immersion for 5 h was studied. The results are shown in Figures 7 and 8.

It was thus revealed that the surface was strongly damaged (Figure 7) in absence of the inhibitors **4a-d**. Figure 8 demonstrates that the investigated compounds were adsorbed on the steel surface and protect the surface in acidic solution at low concentration ($100 \text{ mg} \times \text{L}^{-1}$), confirming their high inhibition effectiveness.

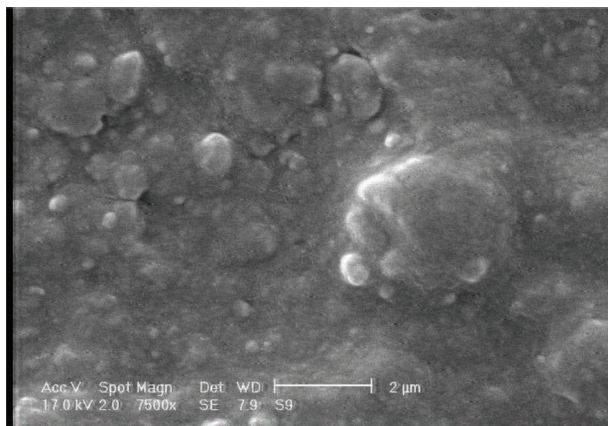


Figure 7. SEM image of surface of carbon steel after immersion for 5 h, 25 °C.

3.6. Antimicrobial activity

To prevent biocorrosion of equipment that is used in the oil industry, various compounds containing active atoms and functional groups in their structures are used [7–10]. Considering this, compounds **4a-d** were studied as biocides for SRB microorganisms at the concentration $50\text{--}200 \text{ mg} \times \text{L}^{-1}$. The results are given in Table 4. According to the experimental results of the antimicrobial activity of **4a-d** against SRB, all the compounds showed bactericidal activity. As shown earlier, the bactericidal activities of the studied compounds depend on their chemical structures. For example, compound **4a**, consisting in the structure chloride ions, has 89% antimicrobial activity at the concentration $200 \text{ mg} \times \text{L}^{-1}$. However, **4b** with bromide anions in the structure has 100% degree at $150 \text{ mg} \times \text{L}^{-1}$. The most actives are **4c** and **4d**. These compounds have 100% degree at $100 \text{ mg} \times \text{L}^{-1}$, probably due to the content of iodide ions in the structures of **4c** and **4d**. In general, the studied compounds have better bactericide effectiveness in comparison with those known [7,10,56].

4. Conclusions

1-(4-(2-Allylphenoxy)butyl)piperidin-1-ium halides **4a-d** were synthesized by the reaction of 1-(4-(2-allylphenoxy)butyl)piperidine with hydrogen halides and ethyl iodide. The compounds were characterized by NMR and FTIR spectra. Synthesized compounds **4a-d** ($50\text{--}150 \text{ mg} \times \text{L}^{-1}$) were studied as corrosion inhibitors in acidic media using the gravimetric and potentiometric methods. It was demonstrated that **4a-d** have high anticorrosion effectiveness for steel St.3 at concentration $150 \text{ mg} \times \text{L}^{-1}$ by gravimetric (84%–95%) and potentiometric (85%–92%) method. The evaluated thermodynamic parameters of adsorption show that compounds **4a-d** are strongly adsorbed on the carbon steel surface, while the SEM images demonstrate good coverage of the surface. Therefore,

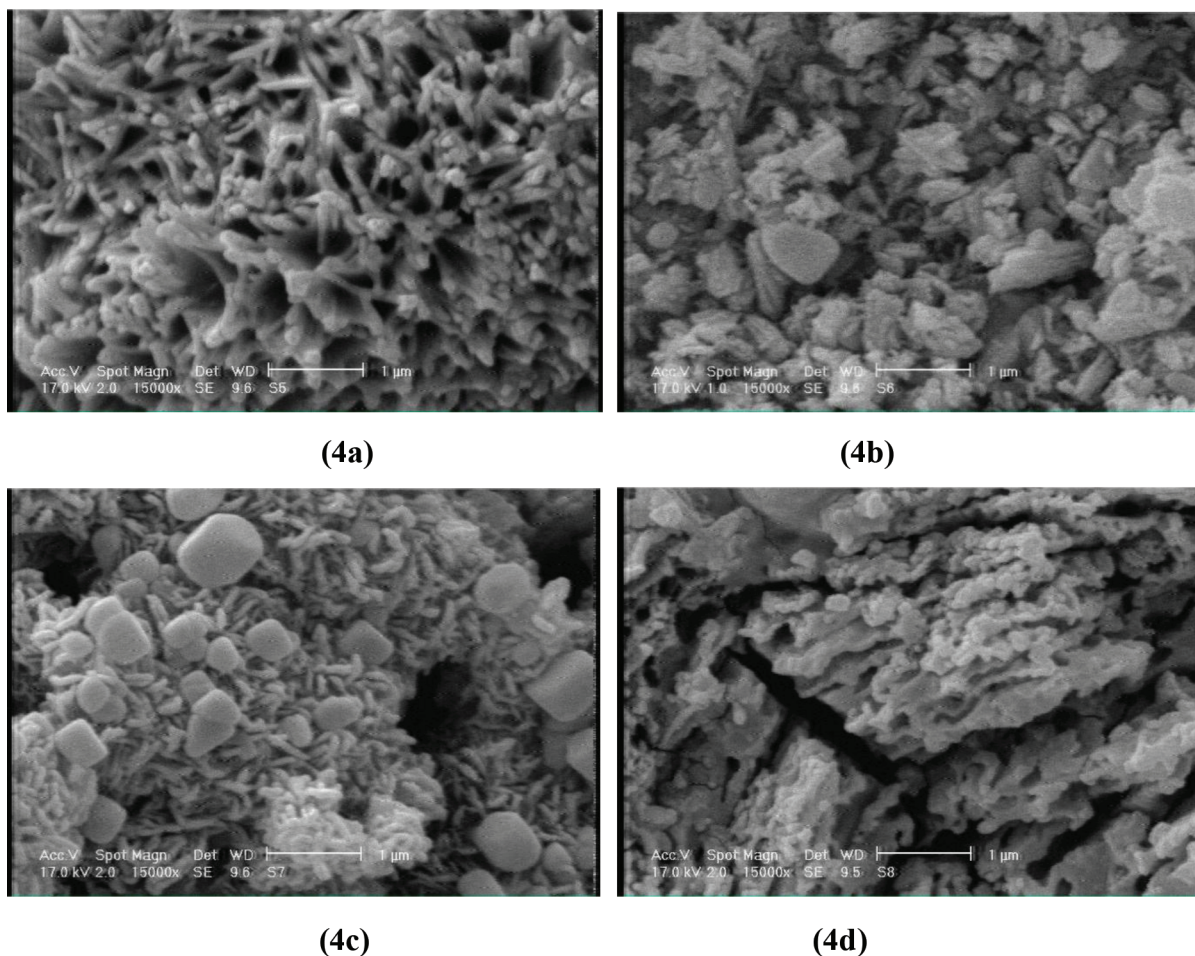


Figure 8. SEM images of surface of carbon steel in the presence of $100 \text{ mg} \times \text{L}^{-1}$ inhibitors **4a-d** for 5 h, 25°C .

the high corrosion inhibition effectiveness can be related to the adherent adsorption of these cationic surfactants on the steel surface and formation of a protective film.

Moreover, **4a-d** were studied as reagents against SRB and their high bactericidal activity (100%) was revealed at concentration $100 \text{ mg} \times \text{L}^{-1}$.

Thus, our study allowed us to conclude that compounds **4a-d** can be used as corrosion inhibitors and biocides. The results show that using such compounds can reduce the rate of metal corrosion and increase their service life.

Acknowledgements

This work was supported by the Science Development Foundation under the President of the Republic of Azerbaijan – Grant No: EIF/MQM/Elm-Tehsil-1-2016-1(26)-71/01/3.

References

1. Tsoeunyane MG, Makhatha ME, Arotiba OA. Corrosion inhibition of mild steel by poly(butylene succinate)-L-histidine extended with 1,6-diisocynatohexane polymer composite in 1 M HCl. International journal of corrosion 2019; Article ID 7406409: 12. doi: 10.1155/2019/7406409

2. Rbaa M, Galai M, Benhiba F, Obot IB, Oudda H et al. Synthesis and investigation of quinazoline derivatives based on 8-hydroxyquinoline as corrosion inhibitors for mild steel in acidic environment: experimental and theoretical studies. *Ionics* 2019; 25: 3473-3491. doi: 10.1007/s11581-018-2817-7
3. Chakravarthy MP, Mohana KN. Adsorption and Corrosion Inhibition Characteristics of Some Nicotinamide Derivatives on Mild Steel in Hydrochloric Acid Solution. *ISRN Corrosion* 2014; Article ID 687276. doi: 10.1155/2014/687276
4. Abd El-Lateef HM, Tantawy AH, Abdelhamid AA. Novel quaternary ammonium-based cationic surfactants: synthesis, surface activity and evaluation as corrosion inhibitors for C1018 carbon steel in acidic chloride solution. *Journal of Surfactants and Detergents* 2017; 20: 735-753. doi: 10.1007/s11743-017-1947-7
5. Abdel Hameed RS, Alfakeer M, Abdallah M. Inhibiting properties of some heterocyclic amide derivatives as potential nontoxic corrosion inhibitors for carbon steel in 1.0 M sulfuric acid. *Surface engineering and applied electrochemistry* 2018; 54: 599-606. doi: 10.3103/S1098375518060054
6. Santos da Silva P, Ferrera de Senna L, Maccado Goncalves MM, Baptista do Lago DC. Microbiologically-influenced corrosion of 1020 carbon steel in Artificial Seawater using garlic oil as natural biocide. *Materials research* 2019; 22: e20180401. doi: 10.1590/1980-5373-MR-2018-0401
7. Manga SS, Oyeleke SB, Ibrahim AD, Aliero AA, Bagudo AI. Influence of bacteria associated with corrosion of metals. *Continental journal of microbiology* 2012; 6: 19-25
8. Badawi AM, Hegazy MA, El-Sawy AA, Ahmed HM, Kamel WM. Novel quaternary ammonium hydroxide cationic surfactants as corrosion inhibitors for carbon steel and as biocides for sulfate-reducing bacteria (SRB). *Materials Chemistry and Physics* 2010; 124: 458-465. doi: 10.1016/j.matchemphys.2010.06.066
9. Kudryavtsev DB, Panteleeva AR, Yurina AV, Lukashenko SS, Khodyrev YP et al. Polymeric inhibitors of hydrogen sulfide corrosion. *Russian Journal of Petroleum Chemistry* 2009; 49 (3): 193-198. doi: 10.1134/S0965544109030025
10. Sikachina A. Polyaminopolyphosphonates and polyaminopolycarbonates (that are chelators) in mission of inhibiting of microbiological corrosion with *Desulfovibrio desulfuricans*. *Bulletin of Science and Practice* 2017; 6: 24-40. doi: 10.5281/zenodo.808189
11. Ashassi-Sorkhabi H, Asghari E, Ejbari P. Electrochemical Studies of Adsorption and Inhibitive Performance of Basic Yellow 28 Dye on Mild Steel Corrosion in Acid Solutions. *Acta Chimica Sloveniya* 2011; 58: 270-277.
12. Vishwanatham S, Haldar N. Furfuryl alcohol as corrosion inhibitor for N80 steel in hydrochloric acid. *Corrosion Science* 2008; 50 (11): 2999-3004. doi: 10.1134/S0965544109030025
13. Offurum FC, Oguzie EE, Offurum JC. Surface response methodology for mild steel corrosion control using udara bark extract as inhibitor. *Continental Journal of Engineering Sciences* 2017; 12 (1): 20-29. doi: 10.5281/zenodo.580792
14. Deivanayagam P, Malarvizhi I, Selvaraj S. Corrosion inhibition efficacy of ethanolic extract of *mimusops elengi* leaves (MEL) on copper in natural sea water. *International Journal of Multidisciplinary Research and Development* 2015; 2 (4): 100-107. doi: 10.22271/ijmrd
15. Abd El Rehim SS, Abdel-Fatah HT, El-Sehiety HE. Inhibitive action of Cystine on the corrosion of low alloy steel ASTM A213 grade T22 in sulfamic acid solutions. *Arabian Journal of chemistry* 2016; 9: 388-394. doi: 10.1016/j.arabjc.2011.05.003
16. Abeng FE, Idim VD, Obonovo OE, Magu TO. Adsorption and adsorption isotherms: application to corrosion inhibition studies of mild steel in 2 M HCl. *World Scientific News* 2017; 77 (2): 298-313.
17. Asassi-Sorkhabi H, Seifzadeh D. Analysis of raw and trend removed EN data in time domain to evaluate corrosion inhibition effects of New Fuchsin dye on steel corrosion and comparison of results with EIS. *Journal of Applied Electrochemistry* 2008; 38 (11): 1545-1552. doi: 10.1007/s10800-008-9602-7

18. Asassi-Sorkhabi H, Seifzadeh D, Hosseini MG. EN, EIS and polarization studies to evaluate the inhibition effect of 3H-phenothiazin-3-one, 7-dimethylamin on mild steel corrosion in 1M HCl solution. *Corrosion Science* 2008; 50 (12): 3363-3370. doi: 10.1016/j.corsci.2008.09.022
19. Asassi-Sorkhabi H, Shaabani B, Seifzadeh D. Effect of some pyrimidinic Schiff bases on the corrosion of mild steel in hydrochloric acid solution. *Electrochimica Acta* 2005; 50: 3446-3452. doi: 10.1016/j.electacta.2004.12.019
20. Al-Novayzer FM, Abdalla M, El-Mossalami EX. N,N-di-(polyoxyethylene)-4-dodecylanyline as corrosion inhibitor for steel in hydrochloric acid solutions. *Russian Journal of Chemistry and Technology of Fuels and Oils* 2012; 6: 453-463. doi: 10.1007/s10553-012-0324-5
21. Sikachina A. Inhibition of corrosion with organic compounds in the water and salt and acid medium. The aspect of isomerism and the interclass aspect of the inhibition process. *Bulletin of Science and Practice* 2018; 4 (1): 10-23. doi: 10.5281/zenodo.1146983
22. Elemike EE, Nwankwo HU, Onwundiwe DC, Hosten EC. Synthesis, structures, spectral properties and DFT quantum chemical calculations of (E)-4-(((4-propylphenyl)imino)methyl)phenol and (E)-4-((2-tolylimino)methyl)phenol; their corrosion inhibition studies of mild steel in aqueous HCl. *Journal of Molecular Structure* 2017; 1141: 12-22. doi: 10.1016/j.molstruc.2017.03.071
23. Batyeva ES, Ugryumov OV, Varnavskaya OA, Khodyrev YuP, Platov EV et al. New, effective carbon dioxide and hydrogen sulfide corrosion inhibitors based on white phosphorus, sulfur, alcohols, and amines. *Russian Journal of Petroleum Chemistry* 2013; 53: 139-143. doi: 10.1134/S0965544113020138
24. Rakhmatullin RR, Levashova VI, Dekhtyar' TF. Synthesis and properties of quaternary ammonium salts on the basis of piperidine. *Russian Journal of Petroleum Chemistry* 2013; 53: 134-138. doi: 10.1134/S0965544113020102
25. Kudryavtsev DB, Panteleeva AR, Yurina AV, Lukashenko SS, Khodyrev YP et al. Polymeric inhibitors of hydrogen sulfide corrosion. *Russian Journal of Petroleum Chemistry* 2009; 49: 193-198. doi: 10.1134/S0965544109030025
26. Veliev MG, Chalabieva AZ, Vezirova IA, Shatirova MI, Gadzhieva MI. Functional derivatives of acetylene as reagents for inhibiting the growth of sulfate-reducing bacteria in oil production. *Russian Journal of Petroleum Chemistry* 2010; 50: 484-488. doi: 10.1134/S0965544110060137
27. Batyeva ES, Ugryumov OV, Varnavskaya OA, Khodyrev YP, Platova EV. New, effective carbon dioxide and hydrogen sulfide corrosion inhibitors based on white phosphorus, sulfur, alcohols, and amines. *Russian Journal of Petroleum Chemistry* 2013; 53: 139-143. doi: 10.1134/S0965544113020138
28. Mekhtiyeva GM, Magerramov AM, Bairamov MR, Agayeva MA, Khoseinzadeh SB et al. Alkenylphenol-based pyridinium salts as hydrogen sulfide corrosion inhibitors and agents for inhibiting the growth of sulfate-reducing bacteria in oil production. *Russian Journal of Petroleum Chemistry* 2015; 55 (3): 247-251. doi: 10.1134/S0965544115030081
29. Maharramov AM, Bairamov MR, Agayeva MA, Mehdiyeva GM, Mammadov IG. Alkenylphenols: preparation, transformation and application. *Russian Chemical Review* 2015; 84: 1258-1278. doi: 10.1070/RCR4437.
30. Maras N, Polane S, Kocevar M. Synthesis of Aryl Alkyl Ethers by Alkylation of Phenols with Quaternary Ammonium Salts. *Acta Chimica Slovenica* 2010; 57 (1): 29-36.
31. Hirschbeck V, Gehrtz PH, Fleischer I. Regioselective thiocarbonylation of vinyl arenes. *Journal of American Chemical Society* 2016; 138 (51): 16794-16799. doi: 10.1021/jacs.6b11020
32. Kohei W, Takashi M, Eri I, Chihiro M, Yasushi Y et al. Hydrazone-Pd-catalyzed direct intermolecular reaction of o-alkenylphenols with allylic acetates. *Organic and Biomolecular Chemistry* 2018; 4 (16): 575-584. doi: 10.1039/C8OB90094
33. Po-Yuan Ch, Yi-Hua W, Mon-Huei H, Tzu-Pin W. Cerium Ammonium Nitrate-Mediated the Oxidative Dimerization of p-Alkenylphenols: A New Synthesis of Substituted (+ -)-trans-Dihydrobenzofurans. *ChemInform* 2013; 69 (2): 653-657. doi: 10.1016/j.tet.2012.11.006

34. Castro AM. Claisen Rearrangement over the Past Nine Decades. *Chemical Review* 2004; 104: 2939-3002. doi: 10.1021/cr020703u
35. Yoshida NC, Benedetti AM, Dos Santos RA, Ramos CS, Batista R et al. Alkenylphenols from *Piper dilatatum* and *P. diospyrifolium*. *Phytochemistry Letters* 2018; 25: 136-140. doi: 10.1016/j.phytol.2018.04.006
36. Horikoshi S, Matsuzaki Sh, Mitani T, Serpone N. Microwave frequency effects on dielectric properties of some common solvents and on microwave-assisted syntheses: 2-Allylphenol and the C₁₂-C₂-C₁₂ Gemini surfactant. *Radiation Physics and Chemistry* 2012; 81: 1885-1895. doi: 10.1016/j.radphyschem.2012. 07.011
37. Krivoruchko EV. Phenolic compounds of *Cornus mas* and *Cornus officinalis*. *Chemistry of Natural Compounds* 2018; 54 (1): 646-647. doi: 10.24959/ubphj.18.151
38. Gavezotti P, Navarra S, Caufin S, Danielli B, Magrone P et al. Synthesis of Enantiomerically Enriched Dimers of Vinylphenols by Tandem Action of Laccases and Lipases. *Advanced Synthesis and Catalysis* 2011; 353: 2421-2430. doi: 10.1002/adsc.201100413
39. Sasano K, Takaya Y, Iwasawa N. Palladium(II)-Catalyzed Direct Carboxylation of Alkenyl C-H Bonds with CO₂. *Journal of American Chemical Society* 2013; 135: 10954-10957. doi: 10.1021/ja405503y
40. Musalov MV, Ishigeev RS, Udalova SI, Musalova MV, Kurkutov EO et al. Synthesis of fused compounds on the basis of chalcogen chlorides and 2-allylphenols. *Russian Journal of Organic Chemistry* 2018; 54: 1035-1040. doi: 10.1134/S1070428018070114
41. Maharramov AM, Bairamov MR, Mehdiyeva GM, Hoseinzadeh SB, Askerov RK. 1,4-Bis[2-(prop-1-enyl)phenoxy] butane. *Acta Crystallographica Section E* 2011; 67: o1478. doi: 10.1107/S1600536811018538
42. Maharramov AM, Bairamov MR, Mehdiyeva GM, Hoseinzadeh SB, Rashidov BA. 1,10-Bis[2-(prop-1-enyl)phenoxy] decane. *Acta Crystallographica Section E* 2012; E68: o266. doi: 10.1107/S1600536811055061
43. Qu T, Zhang J, Meng Z, Liu X, Cao Y et al. Metabolism of fungicide 2-allylphenol in *Rhizoctonia cerealis*. *Ecotoxicology and Environmental Safety* 2014; 102: 136-141. doi: 10.1016/j.ecoenv.2014.01.025
44. Maharramov AM, Bairamov MR, Hoseinzadeh ShB, Agayeva MA, Mehdiyeva GM et al. Synthesis of hydrogen sulfide corrosion inhibitors for oil production. *Russian journal of Petroleum Chemistry* 2013; 53 (6): 423-425. doi: 10.1134/S0965544113060121
45. Rani R, Arora S, Kaur J, Kumari M. Phenolic compounds as antioxidants and chemopreventive drugs from *Streptomyces cellulosa* strain TES17 isolated from rhizosphere of *Camellia sinensis*. *BMC Complementary and Alternative Medicine* 2018; 18 (1): 82-86. doi: 10.1186 /s12906-018-2154-4
46. Maharramov AM, Bairamov MR, Mehdiyeva GM, Agayeva MA. Study of radical copolymerization of aminomethylated derivatives of alkenylphenols with styrene. *Russian Journal of Polymer Science B* 2012; 54 (7-8): 399-406. doi: 10.1134/ S1560090412080039
47. Maharramov AM, Bayramov MR, Mehdiyeva GM, Agayeva MA, Mammadova PS et al. Synthesis of aminomethylated derivatives of allylphenols and study of their antimicrobial characteristics in motor oil. *Russian Journal of Applied Chemistry* 2007; 80: 665-668. doi: 10.1134/S1070427207040295
48. Maharramov AM, Bayramov MR, Mehdiyeva GM, Agayeva MA, Mammadova PS et al. Study of aminomethylation derivatives of allylphenols as antimicrobial additives for TS-1 jet fuel. *Russian Journal of Petroleum Chemistry* 2008; 48: 63-66. doi: 10.1134/S096554410801012X
49. Maharramov AM, Bayramov MR, Mehdiyeva GM, Abushev RA, Agayeva MA et al. Aminomethylated derivatives of 2-propenyl- and 4-isopropenylphenols as antimicrobial additives for petroleum products. *Russian Journal of Petroleum Chemistry* 2010; 50: 69-73. doi: 10.1134/S096554411001010X
50. Vicca P, Steudel S, Smout S, Raats A, Genoe J et al. Interlayer Processing for Active Matrix Organic Light Emitting Diode (OLED) Displays. *Thin Solid Films* 2010; 519: 391-393. doi: 10.5772/19376

51. Chiu CJ, Pei ZW, Chang SP, Chang SJ. Influence of weight ratio of poly(4-vinylphenol) insulator on electronic properties of InGaZnO thin-film transistor. *Journal of Nanomaterials* 2012 (2012) Art.ID 698123. doi: 10.1155/2012/698123
52. Bairamov MR, Magerramov AM, Aliyev IA, Hosseinzadeh ShB, Mehdiyeva GM. Study of 2-allylphenol with symmetric dibromo(C1-C2)alkanes. *Elmi Eserler — Fundamental Elmler*. 2011; 37: 128-130.
53. RD 39-0147-103-350-89: Methodology for monitoring microbiological contamination of oilfield waters and evaluating the protective and bactericidal action of reagents. Ufa, Russia: VNISSPTneft, 1989, pp. 21.
54. Hamadi L, Mansouri S, Oulmi K, Kareche A. The use of amino acids as corrosion inhibitors for metals: a review. *Egyptian Journal of Petroleum* 2018; 27: 1157-1165. doi: 10.1016/j.ejpe.2018.04.004
55. Mohan R, Joseph A. Corrosion protection of mild steel in hydrochloric acid up to 313 K using propyl benzimidazole: Electroanalytical, adsorption and quantumchemical studies. *Egyptian Journal of Petroleum* 2018; 27: 11-20. doi: 10.1016/j.ejpe.2016.12.003
56. Vekantesh R, Geetha K. Synthesis, characterization and antimicrobial activity of nickel (II) complexes derived from pentadentate schiff base. *International Journal of Applied and Advanced Scientific Research*. 2017; 2 (1): 94-98. doi: 10.5281/zenodo.259868